



Published in final edited form as:

*Biomaterials*. 2019 November ; 222: 119441. doi:10.1016/j.biomaterials.2019.119441.

## Synthesis of a Long Acting Nanoformulated Emtricitabine ProTide

Dhruvkumar Soni<sup>a,b</sup>, Aditya N. Bade<sup>b</sup>, Nagsen Gautam<sup>a</sup>, Jonathan Herskovitz<sup>b</sup>, Ibrahim M. Ibrahim<sup>b</sup>, Nathan Smith<sup>b</sup>, Melinda S. Wojtkiewicz<sup>b</sup>, Bhagya Laxmi Dyavar Shetty<sup>b</sup>, Yazen Alnouti<sup>a</sup>, JoEllyn McMillan<sup>b</sup>, Howard E. Gendelman<sup>a,b,\*</sup>, Benson J. Edagwa<sup>b,\*</sup>

<sup>a</sup>Department of Pharmaceutical Sciences, University of Nebraska Medical Center, Omaha, NE 68198 USA

<sup>b</sup>Department of Pharmacology and Experimental Neuroscience, University of Nebraska Medical Center, Omaha, NE 68198 USA

### Abstract

While antiretroviral therapy (ART) has revolutionized treatment and prevention of human immunodeficiency virus type one (HIV-1) infection, regimen adherence, viral mutations, drug toxicities and access stigma and fatigue are treatment limitations. These have led to new opportunities for the development of long acting (LA) ART including implantable devices and chemical drug modifications. Herein, medicinal and formulation chemistry were used to develop LA prodrug nanoformulations of emtricitabine (FTC). A potent lipophilic FTC phosphoramidate prodrug (M2FTC) was synthesized then encapsulated into a poloxamer surfactant (NM2FTC). These modifications extended the biology, apparent drug half-life and antiretroviral activities of the formulations. NM2FTC demonstrated a > 30-fold increase in macrophage and CD4+ T cell drug uptake with efficient conversion to triphosphates (FTC-TP). Intracellular FTC-TP protected macrophages against an HIV-1 challenge for 30 days. A single intramuscular injection of NM2FTC, at 45 mg/kg native drug equivalents, into Sprague Dawley rats resulted in sustained prodrug levels in blood, liver, spleen and lymph nodes and FTC-TP in lymph node and spleen cells

**\*Co-corresponding authors:** Howard E. Gendelman, M.D., Department of Pharmacology and Experimental Neuroscience, University of Nebraska Medical Center, Omaha, NE 68198-5880, USA; phone: 402-559-8920; fax: 402-559-3744; hegendel@unmc.edu and Benson Edagwa, Ph.D., Department of Pharmacology and Experimental Neuroscience, University of Nebraska Medical Center, Omaha, NE 68198-5800, USA; phone: 402-559-3093; fax: 402-559-7495; benson.edagwa@unmc.edu. **†Communication author (for submission and review):** Howard E. Gendelman, M.D., Department of Pharmacology and Experimental Neuroscience, University of Nebraska Medical Center, Omaha, NE 68198-5880, USA; phone: 402-559-8920; fax: 402-559-3744; hegendel@unmc.edu.

Author contributions

B.E. – conceived project, study design, design of synthesis and formulation experiments, supervision of experiments, data analysis and interpretation; H.E.G. – conceived project, design of experiments and data interpretation. D.S. – study design, design and execution of most experiments, data acquisition, data analysis and interpretation; A.B. and D.S. co-designed the animal studies and performed the PK experiments in rats. D.S. and J.H. co-designed and developed T-cell assays. N.G., B.S., M.W., and J.M. developed and performed the UPLC/MS/MS analyses. N.G., Y.A., I.L., and N.S. performed data analysis for PK study. H.E.G., B.E., and D.S. wrote the manuscript.

**Conflict of interest:** Declarations of interest: none

Appendix A supplementary data

The authors have no affiliations or financial involvement with any organization or entity with a financial interest in or financial conflict with the subject matter or materials discussed in the manuscript apart from those disclosed. We would like to acknowledge Dr. Kamel Khalili for the gift of the NL4-3 eGFP pseudovirus used in these studies.

**Data Availability:** The raw/processed data required to reproduce these findings cannot be shared at this time due to technical or time limitations.

at one month. In contrast, native FTC-TPs was present for one day. These results are an advance in the transformation of FTC into a LA agent.

## Keywords

Emtricitabine; Prodrug; Formulation; Long-acting slow effective release anti-retroviral therapy (LASER) ART

---

## 1. Introduction

There is an emerging need for long acting (LA) nanoformulations for both treatment and prevention of human immunodeficiency virus type one (HIV-1) infection [1, 2]. Parenteral cabotegravir and rilpivirine (CAB and RPV) LA antiretroviral drug (ARV) formulations [1, 3] and a dapivirine vaginal ring [4] have generated significant enthusiasm and will soon occupy a prominent position in the HIV therapeutic armamentarium [5]. However, there are limitations of each and all of these [6]. They include, but are not limited to, required large injection volumes, site reactions [7], limited viral reservoir drug penetrance [8], cost, limited access [9] and stable drug delivery [10]. While broad numbers of drug-loaded implants and LA nanomedicines are being developed few provide immediate remedies [11]. To these ends our laboratory has focused our efforts on the development of prodrug nanoformulations stabilized by poloxamer surfactants and lipids as LA agents [12, 13]. The rationales are based on extensive past works demonstrating that prodrugs present effective and inexpensive opportunities for improved drug delivery. These include their readily upscale potential and their prior and extensive use as a delivery systems for infectious [14], neuropsychiatric [15] and metabolic disorders [16]. Added to these advantages is the use of the prodrug approach for more than four decades in clinical practice [17–19]. Thus, we contend that parenteral ARV prodrug formulations may be developed as suitable LA injectables. Our works and those of others have offered this track as a creative solution for the current challenges seen in developing LA ARVs as a mainstream HIV treatment strategy.

There are a number of prodrug advantages in the development of LA ARVs. *First*, after physicochemical drug modifications, improvements in drug potency and apparent plasma half-life of the native drug can be realized [18],[20]. *Second*, prodrugs are pharmacologically inactive requiring chemical transformation to produce the parent drug [21] that ensures their retention for extended time periods. This occurs either at the site of injection or in tissue and as such can significantly extend the pool of active drug in plasma and tissue after a single injection. *Third*, prodrugs can positively affect absorption, biodistribution and excretion based on lipophilic and hydrophobic properties. Such modifications of therapeutic compounds facilitates their passive transport across cell and tissue membranes [22]. This also effects depot formation in endosome vesicles [23–25]. *Fourth*, potent ARVs remain underutilized due to their biologic, pharmacokinetic (PK) and pharmacodynamic or physicochemical properties that would benefit from prodrug transformations [26]. Indeed, ARVs that currently have short half-lives with hydrophilic properties provide opportunities for chemical conversions. Conversions from native hydrophilic agents to hydrophobic and lipophilic prodrugs are possible. To these ends, we

developed research platforms to transform existing ARVs into LA agents [27] [12, 13, 28, 29].

ARV potency and bioavailability improvements by production of fatty acid ester prodrugs of nucleoside reverse transcriptase inhibitor (NRTI) compounds were accomplished [28]. Notably and in pursuit of potent LA NRTI inhibitor analogs, design of carbon chain modifications and ProTide strategies were completed. These led to development of a first lipophilic abacavir (ABC) ProTide through screening a range of amino acid and ester promoieties [30]. However, intracellular delivery of LA active drug metabolites remains elusive. Thus, in the present study, we applied a unique LA ProTide nanocrystal strategy to create a LA FTC. We assumed that by bypassing the first phosphorylation step in FTC's intracellular activation pathway could further enhance drug potency. We also reasoned that inclusion of a docosyl phenylalanyl ester in FTC ProTide would confer prodrug nanoparticle stability and would enhance intracellular delivery of the nucleoside monophosphates [31]. Once cleaved, docosanol would promote drug-drug synergy [32, 33].

## 2. Materials and Methods

### 2.1. Materials

All chemical synthesis reactions were performed under a dry argon atmosphere unless otherwise noted. Reagents were obtained from commercial sources and used directly; exceptions are noted. FTC was purchased from HBCChem (Fremont, CA). Phenyl dichlorophosphate, N-(carbobenzyloxy)-L-phenylalanine, docosanol, dichloromethane (DCM, CH<sub>2</sub>Cl<sub>2</sub>), chloroform (CHCl<sub>3</sub>), N,N dimethylformamide (DMF), triethylamine (Et<sub>3</sub>N), diethyl ether, tetrahydrofuran (THF), *tert*-Butylmagnesium chloride solution (<sup>t</sup>BuMgCl, 1.0 M in THF), triethylsilane (Et<sub>3</sub>SiH) and methanol were purchased from Sigma-Aldrich (St. Louis, MO). 1-[Bis(dimethylamino)methylene]-1H-1,2,3-triazolo[4,5-b]pyridinium 3-oxidhexafluorophosphate (HATU) was obtained from Chem Impex Intl. Inc. (Wood Dale, IL) and palladium, 10% on activated carbon was purchased from STREM Inc. (Newburyport, MA). Flash chromatography was performed using flash silica gel (32–63 μ) from SiliCycle Inc. (Quebec, Canada). Chemical reactions were analyzed by thin layer chromatography (TLC) on precoated silica plates (200 μm, F-254) from Sorbtech technologies Inc. (Norcross, GA). The compounds were visualized by UV fluorescence or by staining with ninhydrin or KMnO<sub>4</sub> reagents. Pyridine, poloxamer 407 (P407), ciprofloxacin, 3-(4,5-dimethylthiazol-2-yl)-2,5-diphenyltetrazolium bromide (MTT), dimethyl sulfoxide (DMSO), paraformaldehyde (PFA), and 3,3'-diaminobenzidine (DAB) were purchased from Sigma-Aldrich (St. Louis, MO). Cell culture grade water (endotoxin free), gentamicin, acetonitrile (ACN), bovine serum albumin (BSA), and LC-MS-grade water were purchased from Fisher Scientific (Hampton, NH). Heat-inactivated pooled human serum was purchased from Innovative research (Novi, MI). Phosphatase, acid from sweet potato (P1435–500UN) was purchased from Sigma Aldrich. Dulbecco's Modification of Eagle's Medium (DMEM) was purchased from Corning Life Sciences (Tewksbury, MA) and RPMI 1640-L-glutamine (SKU# 11875–093) was purchased from Gibco, ThermoFisher Scientific. LiveDead Fixable Blue Dead Cell Stain kit was purchased from Invitrogen,

ThermoFisher. CEM-ss CD4<sup>+</sup> T-cells were obtained from the National Institutes of Health cell repository.

## 2.2. Synthesis of a phosphorylated FTC prodrug

FTC (1.5 g, 6.02 mmols, 1 equivalent) was dried from anhydrous pyridine (15 mL), resuspended in anhydrous THF (30 mL) and then cooled at  $-78^{\circ}\text{C}$  under an argon atmosphere.  $t\text{BuMgCl}$  (12.04 mmols, 2 equivalents) was then added and allowed to stir for 15 minutes under protection from light. A solution of phenylalanine docosyl phosphochloridate [30] (3.89 g, 6.02 mmols, 1 equivalent) in THF (20 mL) was then added dropwise to the anion at  $-78^{\circ}\text{C}$ . The reaction mixture was gradually warmed to room temperature for 1 day and heated at  $45^{\circ}\text{C}$  for 24 h. The mixture was then cooled at  $-78^{\circ}\text{C}$  and quenched using methanol and concentrated to remove solvents. The residue was purified by silica column flash chromatography eluting with 95% then 90% DCM in methanol to give M2FTC as a colorless powder after lyophilization (61 % yield). The chemical structure of M2FTC was confirmed by proton, carbon and phosphorus nuclear magnetic resonance ( $^1\text{H}$ ,  $^{13}\text{C}$  and  $^{31}\text{P}$  NMR) spectra recorded on a Varian Unity/Inova-500 NB (500 MHz; Varian Medical Systems Inc., Palo Alto, CA, USA) (Supplementary Fig. 1 (A, B, C)). FT-IR analysis was performed on a Spectrum Two FT-IR spectrometer (PerkinElmer, Waltham, MA, USA). Comparative crystallographic analyses of FTC and M2FTC by powder X-ray diffraction (XRD) were carried out in the  $2\theta$  range of  $2-500$  using PANalytical Empyrean diffractometer (PANalytical Inc., Westborough, MA, USA) with Cu-K $\alpha$  radiation ( $1.5418 \text{ \AA}$ ) at 40 kV, 45 mA setting. FTC and M2FTC quantitation was performed on a Waters ACQUITY ultra performance liquid chromatography (UPLC) H-Class System with TUV detector and Empower 3 software (Milford, MA, USA) using a Phenomenex Kinetex  $5 \mu\text{m}$  C18  $100 \text{ \AA}$  column (150, 4.5 mm) (Torrence, CA) for separation. Molecular mass was determined by direct infusion into a Waters TQD mass spectrometer. The UPLC-TUV and mass spectrometric methods for FTC and M2FTC quantitation are included in the supplementary information.

## 2.3. M2FTC characterization

**2.3.1. Solubility**—To determine solubility of FTC and M2FTC in water and 1 – octanol, excess amount of drug was added to each media to form saturated solutions. The homogeneous saturated solutions were mixed at room temperature for 24 h and centrifuged at  $14,000 \times g$  for 10 minutes to separate insoluble drug. The amount of drug in the supernatants was quantified by UPLC TUV method.

**2.3.2. Prodrug chemical stability**—Chemical stability at acid, alkaline and neutral pH was determined as described by Gupta et al. [34]. M2FTC stock solution at a concentration of 2 mg/mL was prepared in optima-grade methanol in a glass amber vial. For acidic, alkaline and neutral hydrolysis, 100  $\mu\text{L}$  of M2FTC stock solution was added to 1900  $\mu\text{L}$  each of 0.1 M HCl, 0.1 M NaOH or optima-grade water, respectively. The samples were then incubated at room temperature under shaking conditions (innova® 42 shaker incubator, 150 rpm). Samples were withdrawn at predetermined time points (0, 4, 8 h and 1, 3 and 7 days) and stored at  $-80^{\circ}\text{C}$  until analysis by UPLC-TUV.

**2.3.3. Plasma stability**—To evaluate prodrug stability, 100  $\mu\text{L}$  plasma from different species (rat, mouse, rabbit, dog, monkey and human) were incubated with 1  $\mu\text{M}$  of M2FTC at 37 °C. At different time points (0, 2, 6, and 24 h), 1 mL methanol was added to each sample and vortexed for 3 min to stop the reaction. For 0-min time-point, a 100  $\mu\text{L}$  ice cold plasma was spiked with 100-x prodrug spiking solution in 20%DMSO/80% methanol and immediately 1 ml of ice cold methanol was added. Heat-inactivated plasma was incubated at the same conditions and used as a negative control to differentiate chemical vs. biological instability. Following the addition of methanol, samples were centrifuged at 15,000 g for 10 min, 10  $\mu\text{L}$  supernatant was mixed with 90  $\mu\text{L}$  80 % methanol containing IS, and then 10  $\mu\text{L}$  was used for UPLC-MS/MS analysis (Waters Xevo TQ-XS, supplemental method S.M.1).

## 2.4. Nanoformulation of M2FTC and physicochemical characterization

P407 stabilized M2FTC nanosuspensions (NM2FTC) were prepared by high-pressure homogenization on an Avestin EmulsiFlex-C3 (Ottawa, ON, Canada) homogenizer. Specifically, P407 (0.5% w/v) was dissolved in PBS followed by addition of M2FTC (1% w/v) to the surfactant solution at a drug to polymer ratio of 2:1 and mixed to form a pre-suspension. The suspension was then homogenized (~20,000 psi) until the desired particle size was achieved. Particle size ( $D_{\text{eff}}$ ), polydispersity index (PDI), and zeta potential were determined by dynamic light scattering (DLS) on a Malvern Nano-ZS (Worcestershire, UK). The stability of NM2FTC nanoparticles was monitored at 25 and 37 °C over 2 months. Encapsulation efficiency was calculated using the following equation: Encapsulation efficiency (%) = (weight of drug in formulation/initial weight of drug added)  $\times$  100. In-vitro nanoparticle release kinetics were determined by dialysis (membrane MWCT 2000, Spectrum laboratories, Inc.) against PBS containing 1% v/v Tween 80 at 37 °C with constant shaking (New Brunswick™ Innova® 42, 150 rpm). One milliliter aliquots were withdrawn at predetermined time points and replaced with equal amounts of dispersion medium. Samples were then centrifuged at 10,000 $\times$ g for 10 min and then lyophilized followed by reconstitution in 100  $\mu\text{L}$  of methanol and quantification for total M2FTC concentration using LC-MS/MS method using Waters Xevo TQD UPLC MS system, chromatographic separation was performed on a CSH analytical column (2.1 $\times$ 100 mm, 1.7 $\mu\text{m}$ ; Waters) equipped with a guard column (Waters, Milford, MA). Mobile phase A was ammonium formate (10 mM, pH 3.2), while mobile phase B was 100% methanol (mobile phase A: B was 2:98 v/v). The LC method was 7 minutes, run isocratically at 0.35 mL/minute. The following transitions were monitored for M2FTC: m/z 859.19 $\rightarrow$ 229.98 and m/z 859.19 $\rightarrow$ 276.07.

Nanoparticle morphology was analyzed by transmission electron microscopy (TEM). Samples for TEM imaging were fixed by immersion in a solution of 2% glutaraldehyde, 2% paraformaldehyde in a 0.1M Sorenson's phosphate buffer (pH 7.2) at 4 °C for 24 h and processed as previously described [30].

**2.4.1. Cellular drug uptake, retention and triphosphate production in macrophages**—In-vitro characterization of NM2FTC in MDM and CEM-ss CD4+ T-cells was performed as previously described [13, 14, 30, 31, 37] [38]. Human monocytes were obtained by leukapheresis from HIV-1/2 and hepatitis B seronegative donors, and then

purified by counter-current centrifugal elutriation [35]. Human monocytes were plated in 12-well plates at a density of  $1.0 \times 10^6$  cells per well using DMEM supplemented with 10% heat-inactivated pooled human serum, 1% glutamine, 10  $\mu\text{g}/\text{mL}$  ciprofloxacin, and 50  $\mu\text{g}/\text{mL}$  gentamicin. Cells were incubated at 37 °C in a 5% CO<sub>2</sub> incubator. After 7 days of differentiation in the presence of 1000 U/mL recombinant human macrophage colony stimulating factor (MCSF), MDM were treated with 100  $\mu\text{M}$  FTC or NM2FTC. Uptake of drug was assessed by measuring intracellular drug concentrations at 2–8 h after treatment [13]. For drug retention studies, MDM were treated with drug formulations for 8 h with drug formulation then washed 2 times with PBS and maintained with half-media changes every other day until collection from days 1 to 30. For both studies, adherent MDM were washed with PBS, then scraped into PBS, and counted at predetermined time points using an Invitrogen Countess Automated Cell Counter (Carlsbad, CA). Cells were pelleted by centrifugation at 3,000 rpm for 8 min at 4°C. The cell pellets were then sonicated in 200  $\mu\text{L}$  methanol using a probe sonicator to extract drug and centrifuged at 20,000 g for 10 min at 4°C to separate cell debris. FTC and M2FTC drug contents were determined by UPLC-UV/Vis (Supplemental method S.M.1). To assess cell viability, MTT assay was performed [36]. Briefly, MDM were seeded on 96-well plates at a density of  $80.0 \times 10^5$  cells per well and treated with various concentrations (10 – 400  $\mu\text{M}$ ) of FTC or NM2FTC for 6–24 h. After drug treatment, cells were washed twice with PBS and incubated with 100  $\mu\text{L}/\text{well}$  of MTT solution (5 mg/mL) for 45 min at 37 °C. After incubation MTT was removed, and 200  $\mu\text{L}/\text{well}$  of DMSO was added and mixed thoroughly. Absorbance was measured at 490 nm on a Molecular Devices SpectraMax M3 plate reader with SoftMax Pro 6.2 software (Sunnyvale, CA).

**2.4.2. Cellular drug uptake and Triphosphate production in CEM-ss CD4+ T-cell lines**—Twelve-well plates were coated with poly-L-lysine solution (100  $\mu\text{g}/\text{mL}$  in distilled water) for 1 h. Wells were then washed once with sterile water then seeded with CEM-ss cells at a density of  $1 \times 10^6$  cells/well followed by further incubation at 37 °C for at least 30 minutes. Cells were then treated with 100  $\mu\text{M}$  of FTC or NM2FTC to evaluate drug uptake and retention as previously described [12, 13]. At each time point, cells were washed twice and scrapped into PBS, centrifuged at  $650 \times g$  for 5 minutes and intracellular drug quantitation was performed using TQD MS method as previously described. To determine intracellular FTC triphosphate (FTC-TP) levels, CEM-ss CD4+ T-cells were treated with 100  $\mu\text{M}$  FTC or NM2FTC and processed as described for uptake [43]. Cell pellets were suspended in 70% aqueous methanol (v/v) and FTC-TP extraction was performed as described previously with some modifications [32]. Briefly, Sep-Pak QMA cartridges were used to separate FTC-TP from its mono- and di-phosphate forms. The triphosphate fractions were eluted and dephosphorylated using type XA sweet potato acid phosphatase. The <sup>15</sup>N<sub>2</sub><sup>13</sup>C-3TC internal standard was added following the incubation (final concentration of 0.5 ng/mL). Dephosphorylated samples were then subjected to 2<sup>nd</sup> SPE extraction step using Waters OASIS HLB cartridges. The FTC were then eluted with 1.4 ml of methanol and evaporated under vacuum. Once dry, the residues were reconstituted with 100  $\mu\text{L}$  25% methanol before performing LC–MS/MS analyses as described in the supplemental method S.M.1.



#### 2.4.3. Half maximum effective concentration (EC<sub>50</sub>) measurements—MDM

were seeded in round bottom 96 well plates at a density of 80,000 cells/well. Various concentrations of NM2FTC or FTC in the range of 0.01 nM-10  $\mu$ M were added for 60 min prior to infection with HIV-1<sub>ADA</sub> media at a MOI of 0.1 infectious particles per cell for 4 h. After 4 h, infection media was removed, and the cells were incubated an additional 10 days in the presence of the same concentration of drug. Half media changes were done every other day. After 10 days, culture media was collected to measure HIV-1 reverse transcriptase (RT) activity as previously described [37–39]. Parallel studies were performed in transformed CD4+ T cells. Briefly, CEM-CD4+ T cells were cultured in suspension in 96 well plates, centrifuged at 650  $\times$  g and re-dispersed in 100  $\mu$ L drug-containing media. After 60 minutes, cells were challenged with HIV-1<sub>NL4-3-eGFP</sub> (MOI 0.1) by spin-inoculation (1125 g for 2 hours, 25°C) followed by incubation in drug-containing media for 16 h. The cells were then washed 3x with PBS to remove extracellular virus and incubated in drug-containing media. Media exchanges occurred every 2 days with drug-containing media. Ten days post HIV-challenge, cell pellets were fixed in 2% PFA and fluorescence was analyzed by flow cytometry. The EC<sub>50</sub> was calculated using sigmoidal 4-point logarithmic regression using GraphPad Prism v7. RT activity was measured in culture media.

#### 2.4.4. Measurements of antiretroviral activities—To assess long-term antiretroviral efficacy, MDM were treated with 100 $\mu$ M NM2FTC or FTC as described above for 8 h.

After treatment, cells were washed with PBS and cultured with fresh media without drug followed by half-media exchanges every other day. At days 1–30 after treatment, cells were challenged with HIV-1<sub>ADA</sub> at a MOI of 0.1 for 16 h. After viral infection, the cells were cultured an additional 7 days with half-media exchanges every other day followed by full media change on the 8<sup>th</sup> day post challenge. Culture fluids were collected on the 10<sup>th</sup> day for measurement of RT activity, while adherent MDM were fixed with 4% PFA and HIV-1p24 protein expression assayed by immunohistochemistry [35, 36].

### 2.5. Pharmacokinetic and biodistribution assessments

All animal studies were approved by the University of Nebraska Medical Center Institutional Animal Care and Use Committee in accordance with the standards incorporated in the Guide for the Care and Use of Laboratory Animals (National Research Council of the National Academies, 2011). Male Sprague Dawley rats (250g; Jackson Labs, Bar Harbor, ME) were maintained on normal diet and water. Animal weights were monitored before the start of the study. The rats were administered a single 45 mg/kg FTC-equivalent dose of FTC or NM2FTC intramuscularly (IM) into the caudal thigh muscle to determine PK over 4 weeks. Blood was collected 2 h and 1, 7, 14, 21, and 28 days. Tissues were collected at days 1, 7, 14 and 28 days. Lymph node cells and splenocytes were isolated on days 1, 7, 14 and 28 days for determination of FTC-TP levels. Prodrug and FTC were quantitated in whole blood and tissue samples by UPLC-MS/MS method (Waters Xevo TQS micro., Milford, MA) (Supplemental method S.M.1).

### 2.6. Statistics

For both in-vitro and in-vivo studies, data were presented as mean  $\pm$  standard deviation (SEM), and experiments were performed using a minimum of three biological replicates. For

in-vivo studies, each group contained 5 rats (pharmacokinetic studies). For comparison of two groups, Student's t-test (two-tailed, paired and unpaired) were used. One way ANOVA was performed for comparison between 3 groups.  $P < 0.05$  was considered to be significant (\* $P < 0.05$ , \*\*\*\* $P < 0.0001$ ). All the data were analyzed using GraphPad Prism 7.0 software (La Jolla, CA).

## 2.7. Study approval

All animal studies were approved by the University of Nebraska Medical Center Institutional Animal Care and Use Committee in accordance with the standards incorporated in the Guide for the Care and Use of Laboratory Animals (National Research Council of the National Academies, 2011). Human monocytes were isolated by leukapheresis from HIV-1/2 and hepatitis seronegative donors according to an approved UNMC IRB exempt protocol.

## 3. Results

### 3.1. Synthesis and characterization of M2FTC

Phenylalanine docosyl ester was reacted with preformed phenyl phosphorodichloridate in the presence of triethylamine (Fig. 1A). This generated a phenylalanyl docosyl ester phosphorochloridate masking group [30]. The amino ester was then coupled with FTC (Fig. 1B) and purified by silica gel column chromatography producing 61% of M2FTC [40]. Nuclear magnetic resonance, Fourier transform infrared spectroscopy and mass spectrometry (NMR, FTIR and MS) confirmed the formation of the prodrug. The M2FTC physicochemical properties consisted of broad singlets at 0.84 ppm and 1.4 ppm and multiplet at 1.1–1.3 ppm in the  $^1\text{H}$  NMR spectrum corresponding to the terminal methyl and symmetrical methylene protons of the fatty alcohol. Additionally, the multiplet at 7.09–7.32 ppm corresponds to the aromatic protons from the aryl and phenylalanine promoieties (Supplemental Fig. 1A).  $^{13}\text{C}$  NMR spectrum of NM2FTC showed additional peaks corresponding to the carbonyl ester (172.2 ppm) and aromatic carbon atoms (124.7, 124.3, 119.9, 119.8 ppm) (Supplemental Fig. 1B).  $^{31}\text{P}$  NMR spectrum of M2FTC demonstrated a dominant single peak (Supplemental Fig. 1C). A 4000-fold decrease in aqueous solubility ( $0.0366 \pm 0.0093$  mg/mL) for M2FTC compared to FTC ( $142.97 \pm 11.24$  mg/mL) was observed. This corresponded to a 90-fold improvement in M2FTC octanol solubility ( $87.56 \pm 0.236$  mg/mL) compared to  $0.97 \pm 0.027$  mg/mL for FTC. These data confirmed the prodrug lipophilicity enhancements ( $p < 0.0001$ ) (Fig. 1C). Additional absorption bands at  $2921 - 2846\text{ cm}^{-1}$  and  $1800 - 1700\text{ cm}^{-1}$  in the FTIR spectrum of M2FTC were seen representing the C-H and C=O stretches in docosanol and phenylalanine esters, respectively (Fig. 1D). XRD spectra confirmed the crystalline nature of M2FTC (Fig. 1E). Changes in the crystallinity of M2FTC compared to FTC was due to conjugation of lipophilic promoieties to the FTC structure during M2FTC synthesis followed by lyophilization, thus affecting its polymorphic form [41, 42]. Infusion of M2FTC into Waters TQD mass spectrometer confirmed a M2FTC molecular ion peak of 859.19 (Supplemental Fig. 1D).



### 3.2. M2FTC chemical stability

Chemical stability for M2FTC was determined at room temperature in buffers of different pH solutions. At neutral pH, M2FTC was stable over 7 days (Supplemental Fig. 2A). However, after 24 h of incubation under acidic and alkaline pH, 10% of the prodrug degraded presumably through ester bond cleavage.

### 3.3. Plasma metabolic stability

The stability of M2FTC was further investigated using plasma from different species. After 24 h of incubation at 37°C, degradation of M2FTC was high in rodent, dog, rabbit and monkey plasma. However, M2FTC remained stable in both normal and heat inactivated human plasma over 24h (Fig. 1F). The observed differences in plasma stability of M2FTC in different species were due to differences in the esterase expression in these tested species [43]. These data sets support the stability of M2FTC in blood for both intracellular and tissue prodrug uptake and FTC triphosphate conversions.

### 3.4. Physical characterization of M2FTC nanoformulations

We next developed stable nanoformulations of the prodrug by a single step scalable nanoparticle manufacturing scheme [44]. P407 stabilized nanosuspensions of M2FTC (NM2FTC) were prepared by high-pressure homogenization with a drug encapsulation efficiency of 70%. Particle size, polydispersity index (PDI), and zeta potential were determined by dynamic light scattering (DLS) and were  $359.4 \pm 13$  nm,  $0.37 \pm 0.02$ , and  $-44.8 \pm 0.2$  mV, respectively. NM2FTC remained stable at 25 and 37 °C (Fig. 2A and Supplemental Fig. 2C) for up to 60 days. The high negative charge provides electrostatic repulsion between the particles to minimize aggregation. Particle dissolution and release of M2FTC from NM2FTC across a dialysis membrane (MWCT 2000) were characterized by an initial burst prodrug release of 40% within 90 minutes. This was followed by sustained release for over 72 h (Supplemental Fig. 2B). Nanoparticle morphologies by TEM showed fairly uniform and spherical particles with diameters less than 400 nm (Fig. 2D) and validated the particle size. Analysis of particle size distribution by size statistical histogram plot employing ImageJ software on TEM images showed 71, 18 and 9 % of the nanoparticle population in the range of 100–250 nm, 250–400 nm and 400–550 nm respectively (Supplemental Fig. 2D) The high drug loading, smaller particle size and minimal excipient usage in NM2FTC nanosuspensions could potentially reduce injection site reactions. HIV-1 RT activity measurements demonstrated that the  $EC_{50}$  of FTC (0.5 nM), M2FTC (0.11 nM), and NM2FTC (0.04 nM) against HIV-1<sub>ADA</sub> in MDM were comparable (one-way ANOVA,  $p=0.74$ ) indicating that conversion of FTC to M2FTC and NM2FTC did not compromise drug potency (Fig. 2B). Similarly, the  $EC_{50}$  of NM2FTC in CEM CD4+ T-cells was not different from FTC (15.55 nM and 25.71 nM, respectively;  $P = 0.5873$ , two tailed t test with Welch correction). These data further confirmed that the antiretroviral activity of the prodrug formulation was not altered by its chemical modification (Fig. 2E). These observations were further confirmed by quantitation of HIV-1<sub>NL4-3</sub> GFP expression on fixed cell samples by flow cytometry (Supplemental Fig. 2E). The reduction in the  $EC_{50}$  for M2FTC was likely due to poor solubility of the hydrophobic prodrug in aqueous culture media. Administration of the prodrug nanoparticles (NM2FTC) with improved dissolution properties confirmed the

expected improvement in drug potency. Since mitochondrial dysfunction is a major adverse effect of NRTIs [45], we performed mitochondrial dehydrogenase activity assessment of FTC, M2FTC and NM2FTC in MDM at 10–400  $\mu\text{M}$  using 3-(4,5-dimethylthiazol-2-yl)-2,5-diphenyltetrazolium bromide (MTT). No effects on mitochondrial reductase activity was observed at all tested drug concentrations. However, M2FTC and NM2FTC exhibited a slight reduction in cell viability above 100  $\mu\text{M}$ , presumably caused by enhanced cellular drug uptake (Fig. 2C). In CEM CD4+ T-cells, neither FTC, M2FTC nor NM2FTC affected cell viability at 200  $\mu\text{M}$  by LiveDead staining (Fig. 2F). Hence, 100  $\mu\text{M}$  drug concentrations were used in subsequent CEM-ss CD4+ T-cell studies. TEM imaging performed in MDM and CEM CD4+ T cells showed NM2FTC within cytoplasmic vesicles. After 8 h of drug treatment, NM2FTC nanoparticles accumulated in cytoplasmic vesicles in both cell lines (Fig. 2G).

### 3.5. Cell based evaluations of NM2FTC particles

**3.5.1. NM2FTC uptake, retention and FTC TP conversion**—NM2FTC was rapidly taken up by MDM and intracellular concentrations increased over 8 h (Fig. 3A). Intracellular drug concentrations were 34.6  $\text{nmoles}/10^6$  cells for NM2FTC and >100-fold higher than FTC (< 0.1  $\text{nmoles}/10^6$  cells) after equimolar drug concentration exposures. NM2FTC was also retained within MDM for up to 30 days (15.9  $\text{nmoles}/10^6$  cells) while native FTC was undetectable at 8 h (Fig. 3B). In order to probe activation of M2FTC inside cells, we quantified intracellular FTC triphosphate (FTC-TP) levels in MDM treated with equivalent concentrations of FTC or M2FTC. For MDM uptake studies, both NM2FTC (28,2541  $\text{fmoles}/10^6$  cells) and FTC (21,7276  $\text{fmoles}/10^6$  cells) produced comparable levels of FTC-TP over the 8 h test period (Fig. 3C). NM2FTC also provided high sustained FTC-TP levels up to day 30 where TP concentration was 312  $\text{fmoles}/10^6$  cells compared to 19.1  $\text{fmoles}/10^6$  cells for FTC (Fig. 3D). Sustained retention of the active TP metabolite from NM2FTC demonstrates slow prodrug release from the nanoparticle then controlled intracellular activation/phosphorylation. Similarly, NM2FTC exhibited enhanced uptake in CEM CD4+ T cells with peak drug concentration of 10,300  $\text{pmoles}/10^6$  cells at 8 h (Fig. 3E). Parallel quantitation of FTC-TP in CEM CD4+ T-cells after single exposure to NM2FTC demonstrated active metabolite levels of  $508.6 \pm 56.14$   $\text{fmoles}/10^6$  cells at 8 h (Fig. 3F). Overall, these data suggest that NM2FTC could be transformed into a long-acting slow-release formulation. Maintaining therapeutic drug levels at cellular sites of infection could potentially disrupt viral replication cycle and prevent further dissemination [46]. Studies performed in human MDM suggest that despite the ability of native ART formulations to achieve high drug concentrations in plasma, viral replication continues to occur due, in part, to restricted drug cell entry across lipid membranes [12, 13]. The inherent lipophilicity of NM2FTC and enhanced intracellular uptake of the prodrug could potentially overcome limitations of native FTC cell delivery.

**3.5.2. Anti-retroviral efficacy**—To assess antiretroviral activity of NM2FTC, MDM were challenged with HIV-1<sub>ADA</sub> for up to 30 days after a single 8 h treatment with 100  $\mu\text{M}$  of the prodrug formulation or native drug. As a result of enhanced MDM drug uptake and sustained retention, NM2FTC exhibited superior antiretroviral activity compared to FTC as measured by HIV RT activity (Fig. 4A) and HIV-1 p24 antigen staining (Fig. 4B). Notably,

complete viral inhibition was maintained for up to 30 days with NM2FTC compared to minimal protection at day one (40%) and no viral inhibition at later time points for FTC treatment (Fig. 4C). The ability of NM2FTC to protect MDM from HIV-1 infection for extended periods of time is a significant step towards transforming FTC into a potent long acting cell and tissue targeted formulation that could be used in pre-exposure prophylaxis or in combination with other long acting ART for HIV-1 treatment.

### 3.6. Pharmacokinetic and biodistribution studies

Male Sprague Dawley (SD) rats were administered a single 45 mg/kg FTC or FTC-equivalent (equimolar FTC) dose of NM2FTC IM into the caudal thigh muscle to determine PK and tissue drug distribution over 4 weeks. Administration of NM2FTC provided sustained high drug levels in blood over four weeks (Fig. 5A). The measured prodrug blood concentrations were  $472.7 \pm 35.4$  ng/mL and  $50 \pm 6.4$  ng/mL at days 1 and 28, respectively. In contrast, native FTC showed rapid drug decay with levels below 2 ng/mL by day 7. Notably, spleen (152 ng/g), liver (79 ng/g) and lymph nodes (152 ng/g) showed high M2FTC concentrations at day 28 (Fig. 5 B–D) with detectable FTC-TP levels (Fig. 5 E, F) all following a single NM2FTC injection. In contrast and like blood, native FTC treatment elicited low drug levels in tissues that rapidly fell below the limit of quantitation (Fig. 5 B–D). The high drug levels in tissues after NM2FTC treatment suggest controlled prodrug release from the nanoparticle with enhanced accumulation of FTC-TP in tissue [47].

## 4. Discussion

Emtricitabine (FTC) is an NRTI with potent activity against HIV-1 and hepatitis B virus (HBV) infections [48, 49]. Daily pre-exposure prophylaxis with a combination of FTC and tenofovir is effective at preventing HIV-1 transmission. Combinations of bicitegravir, emtricitabine and tenofovir alafenamide are a mainline therapy for HIV-1 treatment [50]. Despite its effectiveness, limitations of FTC include regimen adherence and restricted viral reservoir penetrance. These offer the needs for improved formulation strategies. Thus, LA ARV formulations were developed to extend dosing intervals, reduce systemic toxicity, and improve PK profiles [12, 13, 29, 30, 51, 52]. The formulations made were maximized for drug loading and excipient usage. Drug formulation scalability and stability after long-term storage were achieved.

As FTC is highly water-soluble, drug transformation into sustained release solid drug nanocrystals is required. Thus, we designed and applied an optimized ProTide strategy to generate hydrophobic and lipophilic ProTides drug nanocrystals. These extended the drug's apparent half-life through slow nanoparticle dissolution [53] and controlled ProTide hydrolysis and activation [30, 54]. The created FTC prodrug bypassed the initial rate-limiting phosphate kinase activation step and improved its potency. Development of LA nanoformulations with slower hydrolysis rates can sustain therapeutic drug concentrations in plasma and tissue [55] while improving cell penetrance and drug tissue biodistribution [56]. Despite such benefits, only two LA ARVs, RPV and CAB LA, have progressed to phase III clinical trials [3, 57–60]. It is noteworthy that inherent hydrophobicity is critical in creating nanoparticles. However, most ARVs cannot be easily converted into stable aqueous

nanosuspensions [61]. These challenges could be overcome by encapsulation of lipophilic ARV prodrugs into poloxamer coated nanocrystals enabling slow release and hydrolysis rates [12, 13, 28–30].

We reasoned that optimal formulation design should maximize delivery of ART to macrophages and CD4+ T cells, the principal targets of HIV-1 infection, in spleen, gut and lymphoid organ reservoirs. This would improve delivery over native ART nanosuspensions [62] and improve the abilities of highly mobile macrophages with large storage capacities to transfer drug to CD4+ T cells and ultimately to virus tissue compartments [13]. Drugs stored in macrophages as nanocrystals can also protect drugs from systemic metabolism, prolonging drug half-lives to enhance efficacy. Such events would lead to improved PK and drug biodistributions [12, 13]. We have also shown that once inside macrophages, drug particles are stored in late- and recycling-endosomes, as well as autophagosomes [63, 64]. Thus, cell drug delivery serves multiple purposes especially in conjunction with prodrug activation. Activation of ProTides involves protease and peptidase mediated processes to release nucleoside monophosphates, which undergo further phosphorylation into active triphosphate forms [65, 66]. Following intracellular uptake, M2FTC nanocrystal undergo slower dissolution mediated by esterase induced hydrolysis [67–70]. Intracellular M2FTC activation would include cleaving off docosanol from docosyl phenylalanine ester carried out by cathepsin A or carboxyesterases induced ester hydrolysis. This is then followed by intracellular cyclization to form a cyclic intermediate which would then undergo further hydrolysis by phosphoramidase leading to release of FTC monophosphates [50, 71–74]. In All, the creation of NM2FTC significantly improved ProTide stability, enhanced intracellular and sustained delivery of the active triphosphate metabolite compared to native FTC. Consequently, the antiviral activity of the drug was extended from hours to weeks for NM2FTC after single drug treatment of MDM. These results demonstrate that NM2FTC could potentially provide maximal intracellular viral restriction.

Development of optimal therapeutic regimen for effective treatment and prevention of HIV-1 requires sustained delivery of therapeutic drug concentrations in plasma and target tissues [75, 76]. We therefore investigated the abilities of NM2FTC to improve drug PK and biodistribution. A single intramuscular injection of NM2FTC in rats provided sustained and high prodrug concentrations in blood and tissues for one month. In contrast, drug concentrations from FTC treatment declined to undetectable levels within a day. Thus, high intracellular and tissue drug levels for NM2FTC could potentially translate to improved drug efficacy and reduced dosage. Additionally, NM2FTC treated animals showed sustained but low levels of FTC-TP in lymph nodes and spleen at one month compared to undetectable levels for FTC treatment. The observed low FTC triphosphate levels were not surprising since ProTides have been shown to undergo rapid degradation [77] and that cleavage of the phosphoramidate bond could be limited in rodents [78]. Therefore, future PK evaluations should be conducted in non-rodent species. Our data sets are particularly encouraging since evaluation of the prodrug in human macrophages and CD4+ T cells strongly suggest that M2FTC is efficiently metabolized into the active triphosphate form. The developed M2FTC formulation could potentially enhance uptake and sustain therapeutic concentration of FTC TP at restricted reservoirs of infection.

## 5. Conclusions

LA nanomedicines developed for HIV treatment and prevention extend drug half-lives, improve biodistribution and facilitate therapeutic outcomes. The limitations of existing LA ARV parenterals include requirement for frequent dosing, injection site reactions and high injection volumes. Limited distribution of ART within tissue and cellular reservoirs of infection further limits their efficacy. Therefore, new treatment and prevention strategies that permit less frequent dosing, with abilities to sustain therapeutic concentrations of drug at sites of action could potentially improve adherence and reduce transmission of infection. The FTC ProTide formulation described in this work represents a promising approach towards development of a long acting sustained release FTC with improved antiretroviral activity. Single treatment of MDM with NM2FTC demonstrated sustained intracellular FTC-triphosphate levels and antiretroviral activities. PK tests in Sprague Dawley rats demonstrate sustained high drug levels in blood and tissues in NM2FTC treated animals compared to rapid one day drug clearance after native drug treatment. Future studies will evaluate pharmacodynamic profiles of NM2FTC in rhesus macaques and inevitably to evaluations in humans infected or at risk of infection.

## Supplementary Material

Refer to Web version on PubMed Central for supplementary material.

## Acknowledgements

We wish to thank the University of Nebraska Medical Center Cores for Electron Microscopy (Tom Bargar and Nicholas Conoan), NMR Spectroscopy (Ed Ezell), Elutriation and Cell Separation (Myhanh Che and Na Ly) and Comparative Medicine for technical assistance. We would like to acknowledge Temple University and Drs. Won-Bin Young and Kamel Khalili for construction of HIV-1NL4-3-eGFP molecular clone plasmid and T cell assay support, respectively. We thank Drs. Bhavesh Kevadia and Shah Valloppilly of the University of Nebraska for Materials and Nanoscience X-Ray Structural Characterization Facility for support in characterizing the modified antiretroviral drug(s) used in this study. We thank Dr. You Zhou of University of Nebraska Lincoln Center for Biotechnology for carrying out TEM imaging of nanoparticles. The research was supported by the University of Nebraska Foundation, which includes donations from the Carol Swarts, M.D. Emerging Neuroscience Research Laboratory, the Margaret R. Larson Professorship, and the Frances, and Louie Blumkin, and Harriet Singer Endowment, the Vice Chancellor's Office of the University of Nebraska Medical Center for Core Facility Developments and National Institutes of Health grants P01 DA028555, R01 NS36126, P01 NS31492, 2R01 NS034239, P01 MH64570, P01 NS43985, P30 MH062261 and R01 AG043540, 1 R56 AI138613-01A1.

## Abbreviations:

<b>ART</b>	antiretroviral therapy
<b>ARV</b>	antiretroviral
<b>BD</b>	Biodistribution
<b>CAB</b>	cabotegravir
<b>CFM</b>	Chloroform
<b>CEM</b>	human T4-lymphoblastoid cell line
<b>EC<sub>50</sub></b>	half maximal effective concentration

<b>FTC</b>	Emtricitabine
<b>FT-IR</b>	Fourier-transform infrared spectroscopic
<b>HIV-1</b>	human immunodeficiency virus type one
<b>IM</b>	intramuscular
<b>LC-MS</b>	liquid chromatography-mass spectrometry
<b>LPV</b>	lopinavir
<b>MDM</b>	human monocyte-derived macrophage
<b>MOI</b>	multiplicity of infection
<b>MTT</b>	3-(4,5-dimethylthiazol-2-yl)-2,5-diphenyltetrazolium bromide
<b>NM2FTC</b>	nanoformulated emtricitabine ProTide (M2FTC)
<b>PBS</b>	phosphate-buffered saline
<b>PDI</b>	polydispersity index
<b>PFA</b>	paraformaldehyde
<b>PK</b>	pharmacokinetics
<b>ProTide</b>	prodrug nucleotide
<b>RT</b>	reverse transcriptase
<b>TEM</b>	transmission electron microscopy
<b>UPLC-MS/MS</b>	ultraperformance liquid chromatography tandem mass spectrometry
<b>UPLC</b>	ultra-performance liquid chromatography
<b>XRD</b>	X-ray diffraction

## References

- [1]. Barnhart M, Long-Acting HIV Treatment and Prevention: Closer to the Threshold, *Glob Health Sci Pract* 5(2) (2017) 182–187. [PubMed: 2865797]
- [2]. Kovarova M, Benhabbour SR, Massud I, Spagnuolo RA, Skinner B, Baker CE, Sykes C, Mollan KR, Kashuba ADM, Garcia-Lerma JG, Mumper RJ, Garcia JV, Ultra-long-acting removable drug delivery system for HIV treatment and prevention, *Nat Commun* 9(1) (2018) 4156. [PubMed: 30297889]
- [3]. Andrews CD, Heneine W, Cabotegravir long-acting for HIV-1 prevention, *Curr Opin HIV AIDS* 10(4) (2015) 258–63. [PubMed: 26049951]
- [4]. Montgomery ET, van der Straten A, Chitukuta M, Reddy K, Woeber K, Atujuna M, Bekker LG, Etima J, Nakyanzi T, Mayo AJ, Katz A, Laborde N, Grossman CI, Soto-Torres L, Palanee-Phillips T, Baeten JM, Study M-A, Acceptability and use of a dapivirine vaginal ring in a phase III trial, *AIDS* 31(8) (2017) 1159–1167. [PubMed: 28441175]



- [5]. Benitez-Gutierrez L, Soriano V, Requena S, Arias A, Barreiro P, de Mendoza C, Treatment and prevention of HIV infection with long-acting antiretrovirals, *Expert Rev Clin Pharmacol* 11(5) (2018) 507–517. [PubMed: 29595351]
- [6]. Landovitz RJ, Kofron R, McCauley M, The promise and pitfalls of long-acting injectable agents for HIV prevention, *Curr Opin HIV AIDS* 11(1) (2016) 122–8. [PubMed: 26633643]
- [7]. Citrome L, New second-generation long-acting injectable antipsychotics for the treatment of schizophrenia, *Expert Rev Neurother* 13(7) (2013) 767–83. [PubMed: 23898849]
- [8]. Vyas TK, Shah L, Amiji MM, Nanoparticulate drug carriers for delivery of HIV/AIDS therapy to viral reservoir sites, *Expert Opin Drug Deliv* 3(5) (2006) 613–28. [PubMed: 16948557]
- [9]. Tagar E, Sundaram M, Condliffe K, Matatiyo B, Chimbwandira F, Chilima B, Mwanamanga R, Moyo C, Chitah BM, Nyemazi JP, Assefa Y, Pillay Y, Mayer S, Shear L, Dain M, Hurley R, Kumar R, McCarthy T, Batra P, Gwinnett D, Diamond S, Over M, Multi-country analysis of treatment costs for HIV/AIDS (MATCH): facility-level ART unit cost analysis in Ethiopia, Malawi, Rwanda, South Africa and Zambia, *PLoS One* 9(11) (2014) e108304. [PubMed: 25389777]
- [10]. Sosnik A, Chiappetta DA, Carcaboso AM, Drug delivery systems in HIV pharmacotherapy: what has been done and the challenges standing ahead, *J Control Release* 138(1) (2009) 2–15. [PubMed: 19445981]
- [11]. Kirtane AR, Langer R, Traverso G, Past, Present, and Future Drug Delivery Systems for Antiretrovirals, *J Pharm Sci* 105(12) (2016) 3471–3482. [PubMed: 27771050]
- [12]. Zhou T, Su H, Dash P, Lin Z, Dyavar Shetty BL, Kocher T, Szlachetka A, Lamberty B, Fox HS, Poluektova L, Gorantla S, McMillan J, Gautam N, Mosley RL, Alnouti Y, Edagwa B, Gendelman HE, Creation of a nanoformulated cabotegravir prodrug with improved antiretroviral profiles, *Biomaterials* 151 (2018) 53–65. [PubMed: 29059541]
- [13]. Sillman B, Bade AN, Dash PK, Bhargavan B, Kocher T, Mathews S, Su H, Kanmogne GD, Poluektova LY, Gorantla S, McMillan J, Gautam N, Alnouti Y, Edagwa B, Gendelman HE, Creation of a long-acting nanoformulated dolutegravir, *Nat Commun* 9(1) (2018) 443. [PubMed: 29402886]
- [14]. Rautio J, Laine K, Gynther M, Savolainen J, Prodrug approaches for CNS delivery, *AAPS J* 10(1) (2008) 92–102. [PubMed: 18446509]
- [15]. Sozio P, Cerasa LS, Abbadessa A, Di Stefano A, Designing prodrugs for the treatment of Parkinson's disease, *Expert Opin Drug Discov* 7(5) (2012) 385–406. [PubMed: 22494466]
- [16]. Lee JB, Zgair A, Malec J, Kim TH, Kim MG, Ali J, Qin C, Feng W, Chiang M, Gao X, Voronin G, Garces AE, Lau CL, Chan TH, Hume A, McIntosh TM, Soukarieh F, Al-Hayali M, Cipolla E, Collins HM, Heery DM, Shin BS, Yoo SD, Kagan L, Stocks MJ, Bradshaw TD, Fischer PM, Gershkovich P, Lipophilic activated ester prodrug approach for drug delivery to the intestinal lymphatic system, *J Control Release* 286 (2018) 10–19. [PubMed: 30016732]
- [17]. Stella VJ, Nti-Addae KW, Prodrug strategies to overcome poor water solubility, *Adv Drug Deliv Rev* 59(7) (2007) 677–94. [PubMed: 17628203]
- [18]. Ettmayer P, Amidon GL, Clement B, Testa B, Lessons learned from marketed and investigational prodrugs, *J Med Chem* 47(10) (2004) 2393–404. [PubMed: 15115379]
- [19]. Albert A, Chemical aspects of selective toxicity, *Nature* 182(4633) (1958) 421–2. [PubMed: 13577867]
- [20]. Stella VJ, Charman WN, Naringrekar VH, Prodrugs. Do they have advantages in clinical practice?, *Drugs* 29(5) (1985) 455–73. [PubMed: 3891303]
- [21]. Jana S, Mandlekar S, Marathe P, Prodrug design to improve pharmacokinetic and drug delivery properties: challenges to the discovery scientists, *Curr Med Chem* 17(32) (2010) 3874–908. [PubMed: 20858214]
- [22]. Clas SD, Sanchez RI, Nofsinger R, Chemistry-enabled drug delivery (prodrugs): recent progress and challenges, *Drug Discov Today* 19(1) (2014) 79–87. [PubMed: 23993918]
- [23]. Andrews CD, Spreen WR, Mohri H, Moss L, Ford S, Gettie A, Russell-Lodrigue K, Bohm RP, Cheng-Mayer C, Hong Z, Markowitz M, Ho DD, Long-acting integrase inhibitor protects macaques from intrarectal simian/human immunodeficiency virus, *Science* 343(6175) (2014) 1151–4. [PubMed: 24594934]

- [24]. Puligujja P, Balkundi SS, Kendrick LM, Baldrige HM, Hilaire JR, Bade AN, Dash PK, Zhang G, Poluektova LY, Gorantla S, Liu XM, Ying T, Feng Y, Wang Y, Dimitrov DS, McMillan JM, Gendelman HE, Pharmacodynamics of long-acting folic acid-receptor targeted ritonavir-boosted atazanavir nanoformulations, *Biomaterials* 41 (2015) 141–50. [PubMed: 25522973]
- [25]. Kadiu I, Nowacek A, McMillan J, Gendelman HE, Macrophage endocytic trafficking of antiretroviral nanoparticles, *Nanomedicine (Lond)* 6(6) (2011) 975–94. [PubMed: 21417829]
- [26]. Barnhart M, Shelton JD, ARVs: the next generation. Going boldly together to new frontiers of HIV treatment, *Glob Health Sci Pract* 3(1) (2015) 1–11. [PubMed: 25745115]
- [27]. Kudalkar SN, Beloor J, Quijano E, Spasov KA, Lee WG, Cisneros JA, Saltzman WM, Kumar P, Jorgensen WL, Anderson KS, From in silico hit to long-acting late-stage preclinical candidate to combat HIV-1 infection, *Proc Natl Acad Sci U S A* 115(4) (2018) E802–E811. [PubMed: 29279368]
- [28]. Singh D, McMillan J, Hilaire J, Gautam N, Palandri D, Alnouti Y, Gendelman HE, Edagwa B, Development and characterization of a long-acting nanoformulated abacavir prodrug, *Nanomedicine (Lond)* 11(15) (2016) 1913–27. [PubMed: 27456759]
- [29]. Guo D, Zhou T, Arainga M, Palandri D, Gautam N, Bronich T, Alnouti Y, McMillan J, Edagwa B, Gendelman HE, Creation of a Long-Acting Nanoformulated 2',3'-Dideoxy-3'-Thiacytidine, *J Acquir Immune Defic Syndr* 74(3) (2017) e75–e83. [PubMed: 27559685]
- [30]. Lin Z, Gautam N, Alnouti Y, McMillan J, Bade AN, Gendelman HE, Edagwa B, ProTide generated long-acting abacavir nanoformulations, *Chem Commun (Camb)* 54(60) (2018) 8371–8374. [PubMed: 29995046]
- [31]. Piantadosi C, Marasco CJ Jr., Morris-Natschke SL, Meyer KL, Gumus F, Surles JR, Ishaq KS, Kucera LS, Iyer N, Wallen CA, et al., Synthesis and evaluation of novel ether lipid nucleoside conjugates for anti-HIV-1 activity, *J Med Chem* 34(4) (1991) 1408–14. [PubMed: 1901911]
- [32]. Marcelletti JF, Synergistic inhibition of herpesvirus replication by docosanol and antiviral nucleoside analogs, *Antiviral Res* 56(2) (2002) 153–66. [PubMed: 12367721]
- [33]. Katz DH, Marcelletti JF, Pope LE, Khalil MH, Katz LR, McFadden R, n-docosanol: broad spectrum anti-viral activity against lipid-enveloped viruses, *Ann N Y Acad Sci* 724 (1994) 472–88. [PubMed: 8030975]
- [34]. Gupta D, Gupta SV, Lee KD, Amidon GL, Chemical and enzymatic stability of amino acid prodrugs containing methoxy, ethoxy and propylene glycol linkers, *Mol Pharm* 6(5) (2009) 1604–11. [PubMed: 19566080]
- [35]. Gendelman HE, Orenstein JM, Martin MA, Ferrua C, Mitra R, Phipps T, Wahl LA, Lane HC, Fauci AS, Burke DS, et al., Efficient isolation and propagation of human immunodeficiency virus on recombinant colony-stimulating factor 1-treated monocytes, *J Exp Med* 167(4) (1988) 1428–41. [PubMed: 3258626]
- [36]. Mosmann T, Rapid colorimetric assay for cellular growth and survival: application to proliferation and cytotoxicity assays, *J Immunol Methods* 65(1–2) (1983) 55–63. [PubMed: 6606682]
- [37]. Balkundi S, Nowacek AS, Veerubhotla RS, Chen H, Martinez-Skinner A, Roy U, Mosley RL, Kanmogne G, Liu X, Kabanov AV, Bronich T, McMillan J, Gendelman HE, Comparative manufacture and cell-based delivery of antiretroviral nanoformulations, *Int J Nanomedicine* 6 (2011) 3393–404. [PubMed: 22267924]
- [38]. Kalter DC, Nakamura M, Turpin JA, Baca LM, Hoover DL, Dieffenbach C, Ralph P, Gendelman HE, Meltzer MS, Enhanced HIV replication in macrophage colony-stimulating factor-treated monocytes, *J Immunol* 146(1) (1991) 298–306. [PubMed: 1701795]
- [39]. Nowacek AS, McMillan J, Miller R, Anderson A, Rabinow B, Gendelman HE, Nanoformulated antiretroviral drug combinations extend drug release and antiretroviral responses in HIV-1-infected macrophages: implications for neuroAIDS therapeutics, *J Neuroimmune Pharmacol* 5(4) (2010) 592–601. [PubMed: 20237859]
- [40]. McGuigan C, Harris SA, Daluge SM, Gudmundsson KS, McLean EW, Burnette TC, Marr H, Hazen R, Condreay LD, Johnson L, De Clercq E, Balzarini J, Application of phosphoramidate pronucleotide technology to abacavir leads to a significant enhancement of antiviral potency, *J Med Chem* 48(10) (2005) 3504–15. [PubMed: 15887959]

- [41]. Irby D, Du C, Li F, Lipid-Drug Conjugate for Enhancing Drug Delivery, *Mol Pharm* 14(5) (2017) 1325–1338. [PubMed: 28080053]
- [42]. Banerjee S, Kundu A, Lipid-drug conjugates: a potential nanocarrier system for oral drug delivery applications, *Daru* 26(1) (2018) 65–75. [PubMed: 30159763]
- [43]. Bahar FG, Ohura K, Ogihara T, Imai T, Species difference of esterase expression and hydrolase activity in plasma, *J Pharm Sci* 101(10) (2012) 3979–88. [PubMed: 22833171]
- [44]. Zhou T, Lin Z, Puligujja P, Palandri D, Hilaire J, Arainga M, Smith N, Gautam N, McMillan J, Alnouti Y, Liu X, Edagwa B, Gendelman HE, Optimizing the preparation and stability of decorated antiretroviral drug nanocrystals, *Nanomedicine (Lond)* 13(8) (2018) 871–885. [PubMed: 29553879]
- [45]. Kakuda TN, Pharmacology of nucleoside and nucleotide reverse transcriptase inhibitor-induced mitochondrial toxicity, *Clin Ther* 22(6) (2000) 685–708. [PubMed: 10929917]
- [46]. Edagwa BJ, Zhou T, McMillan JM, Liu XM, Gendelman HE, Development of HIV reservoir targeted long acting nanoformulated antiretroviral therapies, *Curr Med Chem* 21(36) (2014) 4186–98. [PubMed: 25174930]
- [47]. Gunawardana M, Remedios-Chan M, Miller CS, Fanter R, Yang F, Marzinke MA, Hendrix CW, Beliveau M, Moss JA, Smith TJ, Baum MM, Pharmacokinetics of long-acting tenofovir alafenamide (GS-7340) subdermal implant for HIV prophylaxis, *Antimicrob Agents Chemother* 59(7) (2015) 3913–9. [PubMed: 25896688]
- [48]. Molina JM, Cox SL, Emtricitabine: a novel nucleoside reverse transcriptase inhibitor, *Drugs Today (Barc)* 41(4) (2005) 241–52. [PubMed: 16034488]
- [49]. Masho SW, Wang CL, Nixon DE, Review of tenofovir-emtricitabine, *Ther Clin Risk Manag* 3(6) (2007) 1097–104. [PubMed: 18516268]
- [50]. Drug and Device News, P T 43(4) (2018) 194–246. [PubMed: 29622938]
- [51]. McMillan J, Szlachetka A, Slack L, Sillman B, Lamberty B, Morse B, Callen S, Gautam N, Alnouti Y, Edagwa B, Gendelman HE, Fox HS, Pharmacokinetics of a Long-Acting Nanoformulated Dolutegravir Prodrug in Rhesus Macaques, *Antimicrob Agents Chemother* 62(1) (2018).
- [52]. Edagwa B, McMillan J, Sillman B, Gendelman HE, Long-acting slow effective release antiretroviral therapy, *Expert opinion on drug delivery* (2017) 1–11.
- [53]. Singh L, Kruger HG, Maguire GEM, Govender T, Parboosing R, The role of nanotechnology in the treatment of viral infections, *Ther Adv Infect Dis* 4(4) (2017) 105–131. [PubMed: 28748089]
- [54]. Sinokrot H, Smerat T, Najjar A, Karaman R, Advanced Prodrug Strategies in Nucleoside and Non-Nucleoside Antiviral Agents: A Review of the Recent Five Years, *Molecules* 22(10) (2017).
- [55]. Edagwa B, McMillan J, Sillman B, Gendelman HE, Long-acting slow effective release antiretroviral therapy, *Expert Opin Drug Deliv* 14(11) (2017) 1281–1291. [PubMed: 28128004]
- [56]. Gautam N, Roy U, Balkundi S, Puligujja P, Guo D, Smith N, Liu XM, Lamberty B, Morse B, Fox HS, McMillan J, Gendelman HE, Alnouti Y, Preclinical pharmacokinetics and tissue distribution of long-acting nanoformulated antiretroviral therapy, *Antimicrob Agents Chemother* 57(7) (2013) 3110–20. [PubMed: 23612193]
- [57]. Trezza C, Ford SL, Spreen W, Pan R, Piscitelli S, Formulation and pharmacology of long-acting cabotegravir, *Curr Opin HIV AIDS* 10(4) (2015) 239–45. [PubMed: 26049948]
- [58]. Jackson A, McGowan I, Long-acting rilpivirine for HIV prevention, *Curr Opin HIV AIDS* 10(4) (2015) 253–7. [PubMed: 26049950]
- [59]. van 't Klooster G, Hoeben E, Borghys H, Looszova A, Bouche MP, van Velsen F, Baert L, Pharmacokinetics and disposition of rilpivirine (TMC278) nanosuspension as a long-acting injectable antiretroviral formulation, *Antimicrob Agents Chemother* 54(5) (2010) 2042–50. [PubMed: 20160045]
- [60]. Williams PE, Crauwels HM, Basstanie ED, Formulation and pharmacology of long-acting rilpivirine, *Curr Opin HIV AIDS* 10(4) (2015) 233–8. [PubMed: 26049947]
- [61]. Rabinow BE, Nanosuspensions in drug delivery, *Nat Rev Drug Discov* 3(9) (2004) 785–96. [PubMed: 15340388]

- [62]. Arainga M, Edagwa B, Mosley RL, Poluektova LY, Gorantla S, Gendelman HE, A mature macrophage is a principal HIV-1 cellular reservoir in humanized mice after treatment with long acting antiretroviral therapy, *Retrovirology* 14(1) (2017) 17. [PubMed: 28279181]
- [63]. Gnanadhas DP, Dash PK, Sillman B, Bade AN, Lin Z, Palandri DL, Gautam N, Alnouti Y, Gelbard HA, McMillan J, Mosley RL, Edagwa B, Gendelman HE, Gorantla S, Autophagy facilitates macrophage depots of sustained-release nanoformulated antiretroviral drugs, *J Clin Invest* 127(3) (2017) 857–873. [PubMed: 28134625]
- [64]. Thomas MB, Gnanadhas DP, Dash PK, Machhi J, Lin Z, McMillan J, Edagwa B, Gelbard H, Gendelman HE, Gorantla S, Modulating cellular autophagy for controlled antiretroviral drug release, *Nanomedicine (Lond)* (2018).
- [65]. Birkus G, Kutty N, He GX, Mulato A, Lee W, McDermott M, Cihlar T, Activation of 9-[(R)-2-[[[(S)-[(S)-1-(Isopropoxycarbonyl)ethyl]amino] phenoxyphosphinyl]-methoxy]propyl]adenine (GS-7340) and other tenofovir phosphonoamidate prodrugs by human proteases, *Mol Pharmacol* 74(1) (2008) 92–100. [PubMed: 18430788]
- [66]. Birkus G, Wang R, Liu X, Kutty N, MacArthur H, Cihlar T, Gibbs C, Swaminathan S, Lee W, McDermott M, Cathepsin A is the major hydrolase catalyzing the intracellular hydrolysis of the antiretroviral nucleotide phosphonoamidate prodrugs GS-7340 and GS-9131, *Antimicrob Agents Chemother* 51(2) (2007) 543–50. [PubMed: 17145787]
- [67]. Jarvis M, Krishnan V, Mitragotri S, Nanocrystals: A perspective on translational research and clinical studies, *Bioeng Transl Med* 4(1) (2019) 5–16. [PubMed: 30680314]
- [68]. Gigliobianco MR, Casadidio C, Censi R, Di Martino P, Nanocrystals of Poorly Soluble Drugs: Drug Bioavailability and Physicochemical Stability, *Pharmaceutics* 10(3) (2018).
- [69]. Gao W, Lee D, Meng Z, Li T, Exploring intracellular fate of drug nanocrystals with crystal-integrated and environment-sensitive fluorophores, *J Control Release* 267 (2017) 214–222. [PubMed: 28844755]
- [70]. Elazzouzi-Hafraoui S, Nishiyama Y, Putaux JL, Heux L, Dubreuil F, Rochas C, The shape and size distribution of crystalline nanoparticles prepared by acid hydrolysis of native cellulose, *Biomacromolecules* 9(1) (2008) 57–65. [PubMed: 18052127]
- [71]. Slusarczyk M, Serpi M, Pertusati F, Phosphoramidates and phosphonamidates (ProTides) with antiviral activity, *Antivir Chem Chemother* 26 (2018) 2040206618775243.
- [72]. Mehellou Y, Rattan HS, Balzarini J, The ProTide Prodrug Technology: From the Concept to the Clinic, *J Med Chem* 61(6) (2018) 2211–2226. [PubMed: 28792763]
- [73]. Prochazkova E, Navratil R, Janeba Z, Roithova J, Baszczynski O, Reactive cyclic intermediates in the ProTide prodrugs activation: trapping the elusive pentavalent phosphorane, *Org Biomol Chem* 17(2) (2019) 315–320. [PubMed: 30543240]
- [74]. Okon A, Han J, Dawadi S, Demosthenous C, Aldrich CC, Gupta M, Wagner CR, Anchimerically Activated ProTides as Inhibitors of Cap-Dependent Translation and Inducers of Chemosensitization in Mantle Cell Lymphoma, *J Med Chem* 60(19) (2017) 8131–8144. [PubMed: 28858511]
- [75]. Pantaleo G, Graziosi C, Demarest JF, Butini L, Montroni M, Fox CH, Orenstein JM, Kotler DP, Fauci AS, HIV infection is active and progressive in lymphoid tissue during the clinically latent stage of disease, *Nature* 362(6418) (1993) 355–8. [PubMed: 8455722]
- [76]. Embretson J, Zupancic M, Ribas JL, Burke A, Racz P, Tenner-Racz K, Haase AT, Massive covert infection of helper T lymphocytes and macrophages by HIV during the incubation period of AIDS, *Nature* 362(6418) (1993) 359–62. [PubMed: 8096068]
- [77]. McGuigan C, Gilles A, Madela K, Aljarah M, Holl S, Jones S, Vernachio J, Hutchins J, Ames B, Bryant KD, Gorovits E, Ganguly B, Hunley D, Hall A, Kolykhalov A, Liu Y, Muhammad J, Raja N, Walters R, Wang J, Chamberlain S, Henson G, Phosphoramidate ProTides of 2'-C-methylguanosine as highly potent inhibitors of hepatitis C virus. Study of their in vitro and in vivo properties, *J Med Chem* 53(13) (2010) 4949–57. [PubMed: 20527890]
- [78]. Song H, Griesgraber GW, Wagner CR, Zimmerman CL, Pharmacokinetics of amino acid phosphoramidate monoesters of zidovudine in rats, *Antimicrob Agents Chemother* 46(5) (2002) 1357–63. [PubMed: 11959569]

### Highlights

1. Creation of emtricitabine (FTC) ProTide nanocrystals
2. A lipophilic FTC phosphoramidate prodrug (M2FTC) was synthesized then encapsulated into a poloxamer surfactant (NM2FTC).
3. NM2FTC demonstrated active macrophage and CD4+ T cells drug uptake of > 30- and 8- fold, respectively.
4. NM2FTC was retained within macrophages for up to a month compared to hours after native FTC treatment.
5. Enhanced potency at half effective concentration ( $EC_{50}$ ) was observed for NM2FTC compared to native FTC in CD4+ T-cells.
6. FTC triphosphates (FTC-TP) were retained in macrophages for one month after a single NM2FTC treatment with associated protection against an HIV-1<sub>ADA</sub> cell challenge of 0.1 infectious viral particles/cell.
7. A single intramuscular injection of NM2FTC, at 45 mg/kg drug equivalents, into Sprague Dawley rats demonstrated sustained prodrug levels in blood, liver, spleen and lymph nodes for up to a month.
8. FTC-TP was detected in cells isolated from lymph nodes and spleen for one month. In contrast, FTC-TPs were present for one day after native drug treatment.

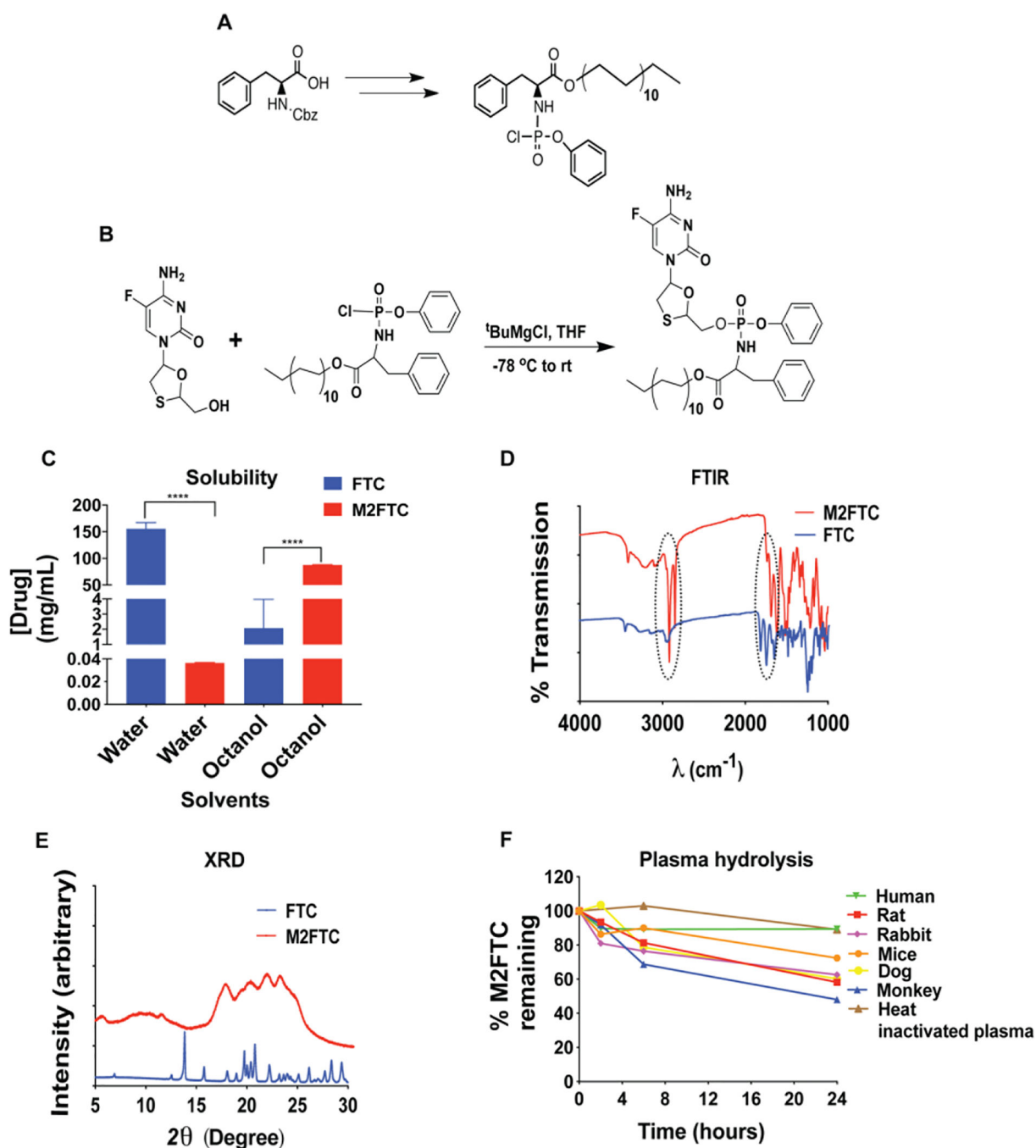


**Fig. 1. M2FTC physicochemical characterization.**

(A) Synthesis of aryl amino phosphochloridate. N-Cbz-L-Phenylalanine was dissolved in DMF and CFM. Cooled on ice. HATU, docosanol, imidazole and Et<sub>3</sub>N were added and reaction was stirred at RT for 48 h. Product was dissolved in CFM and MeOH. Palladium on carbon was added and cooled to 4 °C, Et<sub>3</sub>SiH was added and stirred for 16 h. Product was dissolved in DCM at -78 °C, Phenyl dichlorophosphate was then added, followed by Et<sub>3</sub>N/CFM addition, stirred at 48 h RT. (B) FTC was dissolved in THF at -78 °C, <sup>t</sup>BuMgCl was added and stirred at 48–90 h at RT. FTC was then reacted with product formed in



previous step with a 61% yield **(C)** Solubility of FTC and M2FTC in 1-octanol and water was measured at 37°C. Data are expressed as mean  $\pm$  SEM for n = 3 samples were evaluated. Statistical significance was measured using one way ANOVA at \*\*\*\*P < 0.0001. **(D)** Fourier transformed infra-red spectroscopic (FT-IR) analysis showed the presence of carbonyl and aromatic stretching vibrations in the region of 2900 – 3100 cm<sup>-1</sup> for FTC and M2FTC and phosphoramidate (P-N-H) bending vibrations between 1600 – 1700 cm<sup>-1</sup> in M2FTC, confirming the presence of these functionalities. **(E)** XRD analysis of FTC and M2FTC supporting unique atomic arrangement in the compounds crystal lattice. **(F)** Hydrolysis study in different species' plasma demonstrated chemical stability of M2FTC over 90% in both normal and heat inactivated human plasma up to 24 h at 37 °C and gradual hydrolysis observed of up to 40% in mice and rats, dog, rabbit and in monkey plasma over 24 h.

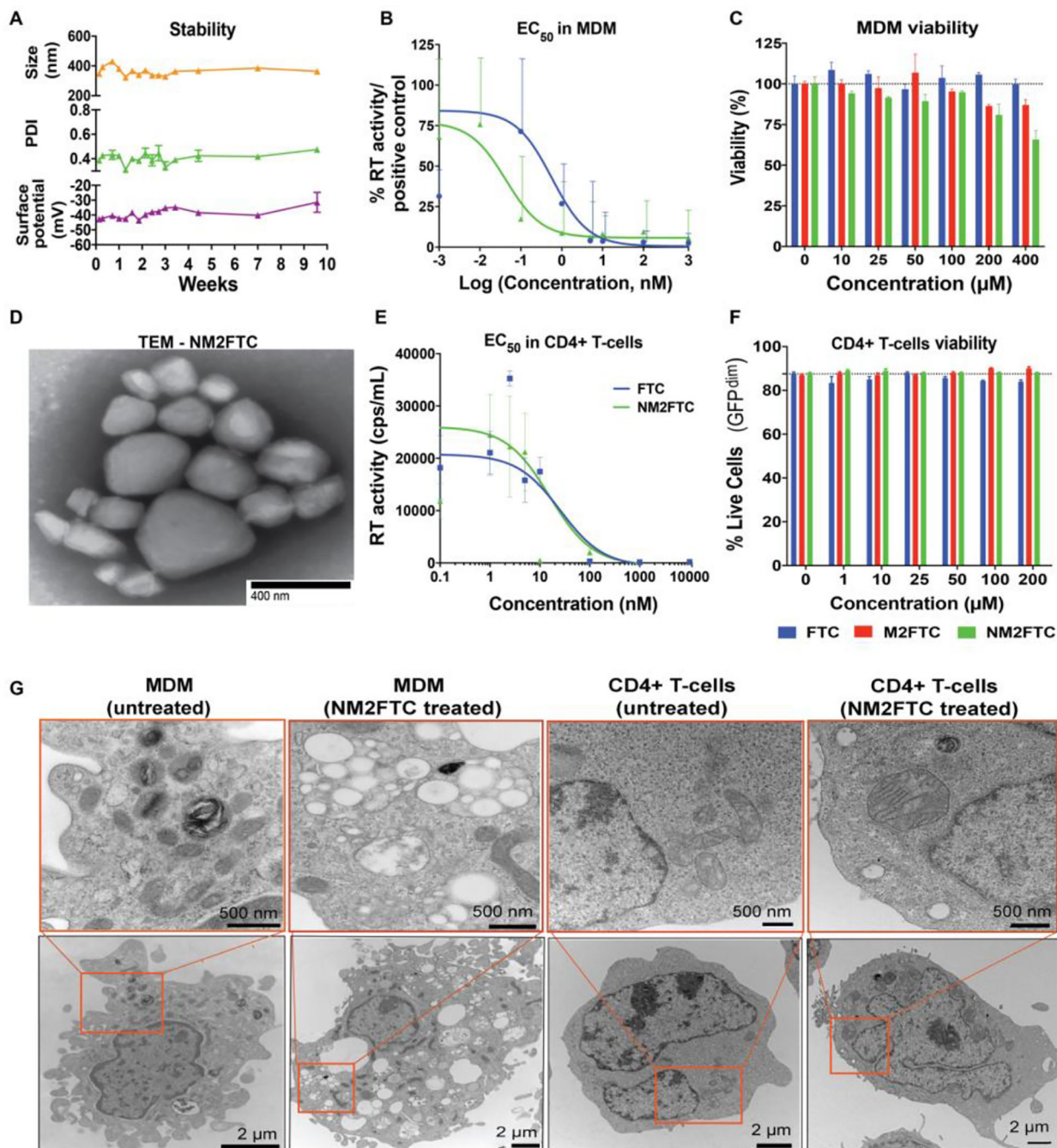


**Fig. 2. NM2FTC characterizations.**

**A)** Physical stability evaluation of NM2FTC at 25 °C in terms of particle size, zeta potential and polydispersity index over 1 month. **(B)** EC<sub>50</sub> was determined in MDM over a range of concentrations (0.001–1000 nM) by determining HIV-1 RT activity after FTC or NM2FTC treatments in cells infected with HIV-1<sub>ADA</sub>. Results were analyzed by nonlinear regression least squares fit. Results are shown as the mean ± SEM of three replicates. **(C)** Cell vitality was assessed in MDM by MTT assay 24 h after FTC, M2FTC or NM2FTC treatments over a range of concentrations (10 – 400 μM). Results were normalized to untreated control cells.

Both M2FTC and NM2FTC were found to be non-cytotoxic at 100  $\mu$ M or less. Data are represented as mean  $\pm$  SEM for n = 3 samples per group. **D)** Transmission electron microscopy (TEM) of NM2FTC showed presence of nanoparticles predominantly in the size range of 100–250 nm. **E)** EC<sub>50</sub> was determined in CEM CD4+ T-cells by RT activity measurement in the supernatant after FTC or NM2FTC treatments over a range of concentrations (0.1–10,000 nM). Results were analyzed by nonlinear regression least squares fit. **F)** CEM-ss CD4+ T-cell vitality using LiveDead staining. All the treatments were non-toxic at 200  $\mu$ M of drug or less. **G)** TEM morphological evaluation in MDM and CEM-ss CD4+ T-cells after NM2FTC (100  $\mu$ M) treatment for 8 h, washing with PBS (2x) and re-suspension in TEM fixation buffer.

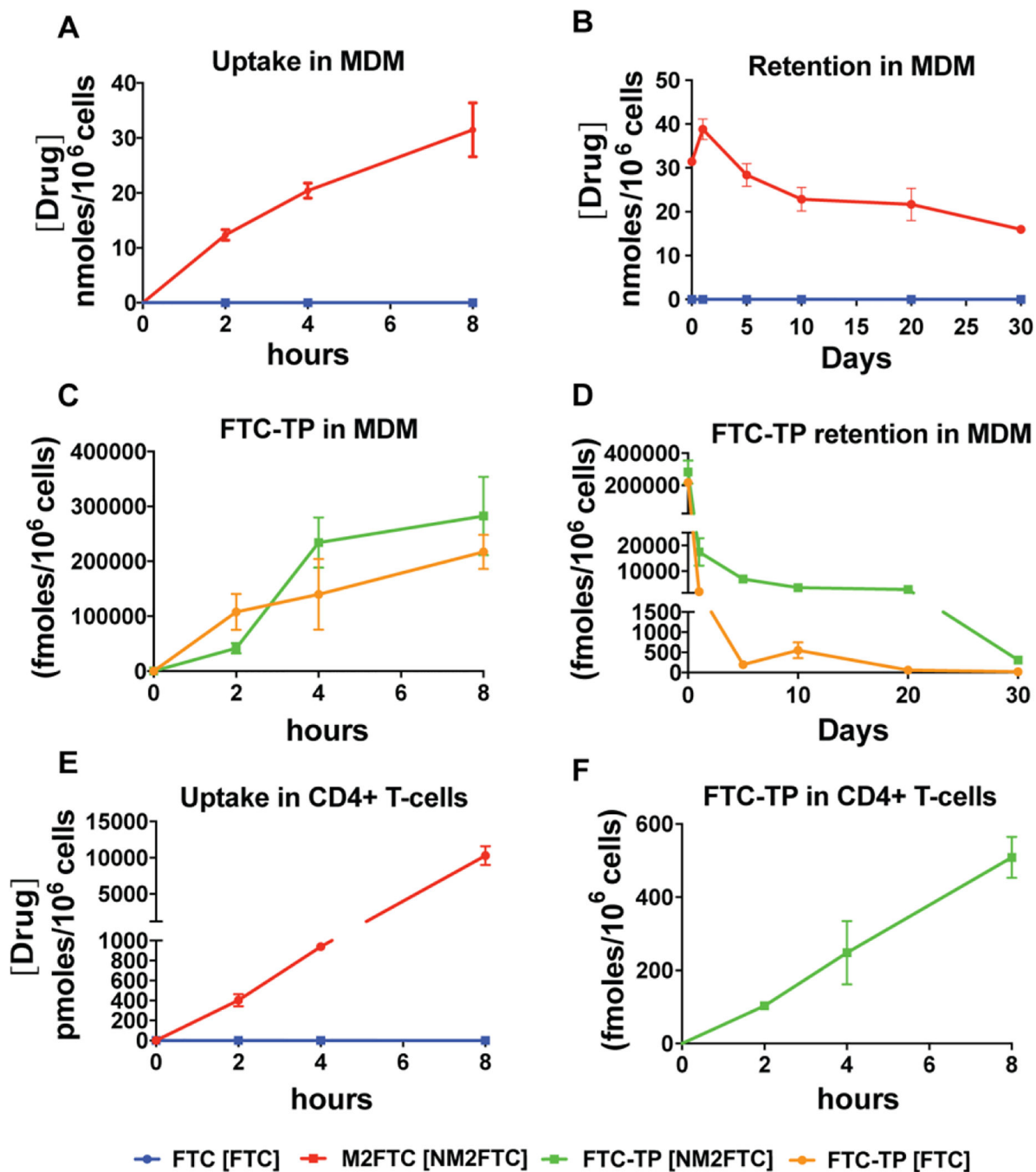


**Fig. 3. NM2FTC uptake, retention and triphosphate (TP) conversion.**

**A)** For uptake, MDM were treated with equal drug concentrations (100  $\mu$ M) and uptake was determined over 8 h. **B)** For retention study, MDM were loaded with FTC or NM2FTC for 8 h followed by PBS washing and maintaining half media changes every other day for 30 days.. **(C)** Intracellular FTC TP levels during uptake studies was quantified at various time points over the 8h experiment time course. **(D)** Intracellular FTC TP levels were measured at different time points over 30-days. **E)** M2FTC, and **F)** FTC TP levels in parallel uptake studies in CEM-ss CD4+ T-cells were carried out as for MDMs.

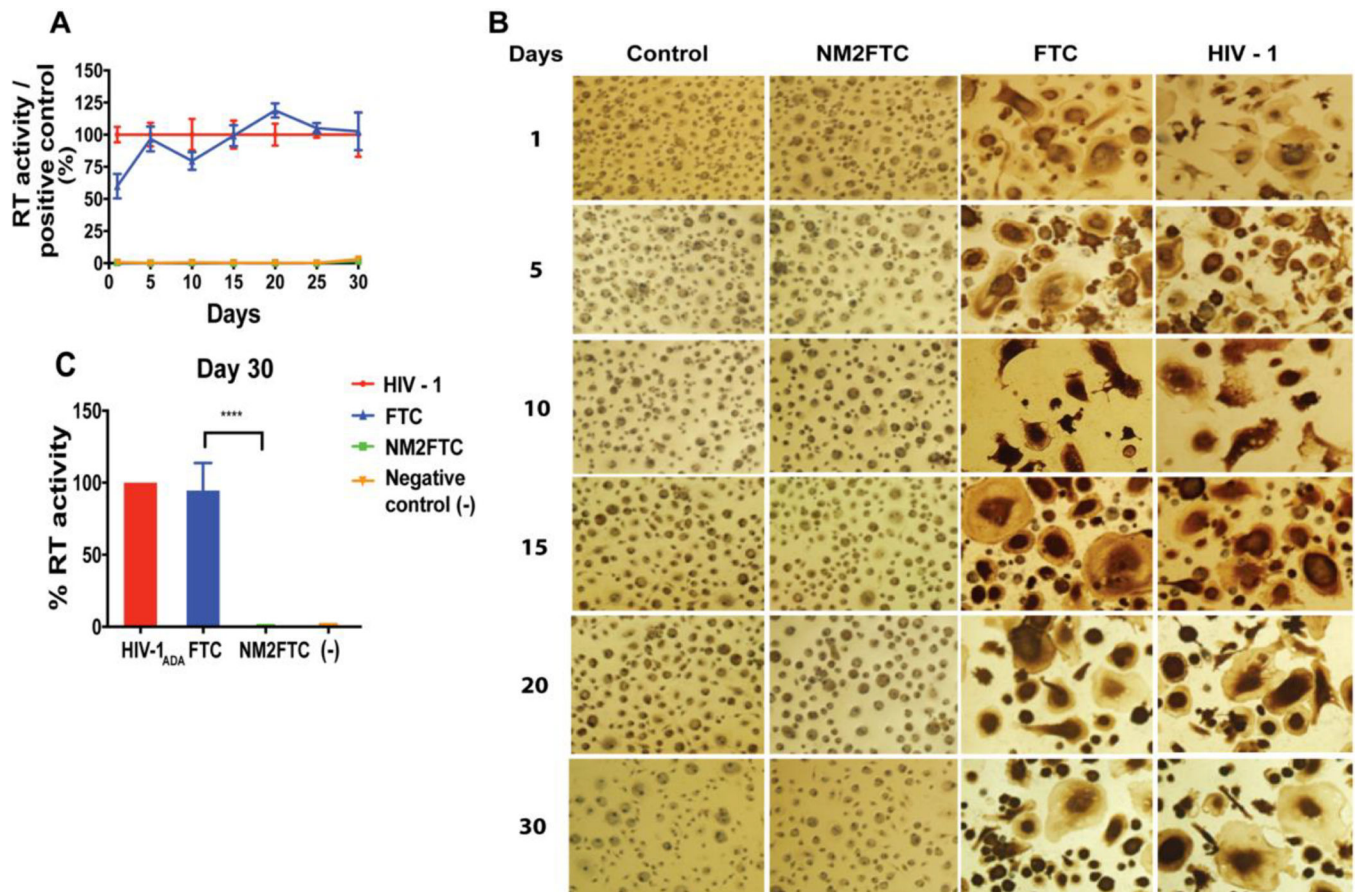


**Fig. 4. Cell-based antiretroviral activities.**

Antiretroviral activity was determined in MDM treated for 8 h with 100  $\mu$ M FTC or NM2FTC and then infected with HIV-1<sub>ADA</sub> at 1 to 30 days following drug loading. HIV-1 replication was determined 10 days after infection by **A**) Time course HIV-1 RT activity in culture supernatants. RT activity results were confirmed by **B**) HIV-1p24 antigen expression (brown stain) of adherent MDM. NM2FTC protected MDM from HIV-1 infection at all time points. Results were normalized to positive control cells. All results are shown as the mean  $\pm$  SEM with  $n = 3$ . **C**) Comparative HIV-1 RT activity at day 30 showing statistical significance in the % RT activity between FTC and NM2FTC treatments using unpaired two tailed t-test at \*\*\*\* $P < 0.0001$ .



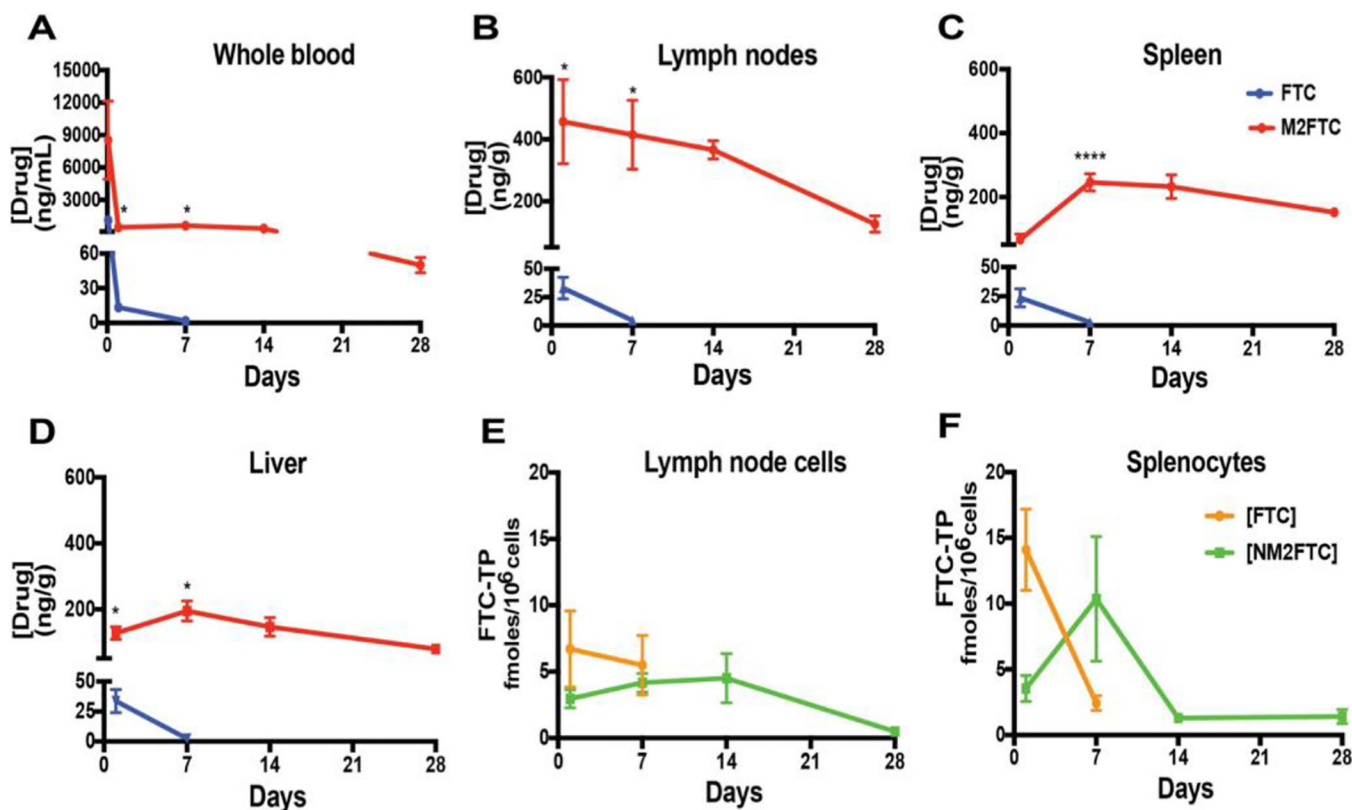


**Fig. 5. PK and biodistribution of FTC and NM2FTC in rats.**

Blood and tissue M2FTC and FTC concentrations were determined over 28 days. **A)** FTC and M2FTC levels in whole blood after a single IM injection of FTC or NM2FTC in Sprague Dawley rats (45 mg/kg FTC equivalents). M2FTC and FTC concentrations were determined in **(B)** lymph nodes, **(C)** spleen, and **(D)** liver. Data are expressed as mean  $\pm$  SEM for  $n = 5$  rats per group. Formation of FTC-TP in **(E)** lymph node and **(F)** splenocytes were determined. Drug concentrations were quantified by UPLC-MS/MS.